SUPPLEMENTAL MATERIAL

SUPPLEMENTAL METHODS

1. Genetic screening of PFHB1

The exon 2 of *GJA5* and exon 3 of *GJC1* that cover the entire coding region of the Cx40 and Cx45, respectively, were amplified by PCR from genome DNA using following primer sets.

GJA5	Forward (Cx40-F2)	5'-TGGAATCCCAGAACATGATAGA-3'
	Reverse (Cx40-R2)	5'-TCAGTTCAGAAGGGACACGTCT-3'
GJC1	Forward (Cx45-F1)	5'-GAGCCACCCTACCCAACTGA-3'
	Reverse (Cx45-R1)	5'-ACCAGAGCCAAATGTTTACTCAA -3'

The coding regions of *KCNQ1*, *KCNH2*, *SCN5A*, *KCNE1*, *KCNE2, KCNJ2, SCN1B, SCN4B, HCN4*, *GJA1* (Cx43) were amplified by PCR using exon flanking intronic primers as previously described.[1-8] Direct DNA sequencing was performed using ABI 3130 genetic analyzer (Applied Biosystems).

2. Plasmid construction

A 1.1-kilobase DNA fragment, encompassing the entire coding region of Cx40, was amplified by PCR from human genomic DNA using the following primers.

Forward (Cx40-F7)	5'-GAAGATCTCACCATGGGCGATTGGAGC TTCCT-3'
Reverse (Cx40-R2X)	5'-GGAATTCACACTGATAGGTCATCTG-3'

(Underlines represent the restriction recognition sequences for BglII and EcoRI, respectively) The PCR fragment was digested with BglII/EcoRI and subcloned into a bicystronic plasmid pIRES2-EGFP or pIRES2-DsRED2 (Takara Bio), for visual identification of cells expressing

connexins and green (EGFP) or red fluorescent protein (DsRED2), respectively. Site-directed mutagenesis was performed by QuikChange (Stratagene) as per manufacturer's instructions. Sequences of PCR-amplified regions were verified for both strands. For EGFP-tagged Cx40 plasmid, the1.1 kb coding sequence of WT and Q58L Cx40 were PCR-amplified by the following primers.

Forward (Cx40-F2X) 5'-AACAAGCTTCACCATGGGCGATTGGAGCTTCCT-3'

Reverse (Cx40-R5X) 5'-GCGGATCCACTGATAGGTCATCTGA-3'

(Underlines represent the restriction recognition sequences for HindIII and BamHI, respectively.) The PCR fragment was digested with HindIII/BamHI and subcloned in frame into the plasmid pEGFP-N1 (Takara Bio), generating fusion constructs (pEGFPN1-Cx40-WT and pEGFPN1-Cx40-Q58L). FLAG-tagged Cx40 plasmids were constructed by replacing the 0.8 kb EGFP fragment of the pEGFPN1-Cx40 plasmids in frame with the FLAG epitope (DYKDDDDK) cDNA at the C-terminal of the Cx40 (pCMV-FLAG-Cx40-WT and pCMV-FLAG-Cx40-Q58L, respectively. EGFP-tag or FLAG-tag did not change the conductance or the gating properties of Cx40 (data not shown).

Bicistronic constructs of WT-Cx40 and Q58L-Cx40 were made using the plasmid pIRES (Takara Bio). The WT-Cx40 (1.1 kb) and EGFP-tagged Q58L-Cx40 (1.8kb) were subcloned either at the upstream or the downstream cloning sites of the IRES (internal ribosomal entry site) (Fig 6B, constructs 3 and 4). Homomeric WT-Cx40 construct and the heteromeric constructs (WT-IRES-Q58L and Q58L-IRES-WT) in Fig 6C were constructed by PCR. WT-Cx40 or Q58L-Cx40 cDNAs were initially PCR-amplified by the primers Cx40-Fa and Cx40-Rb, and the PCR products were digested with NheI/EcoRI and subcloned in the upper multiple cloning sites NheI/EcoRI of pIRES.

Forward (Cx40-Fa) 5'-GCGCTAGCCACCATGGGCGATTGGAGC TTCCT-3'

Reverse (Cx40-Rb) 5'-AGAATTCTCACACTGATAGGTCATCTG-3'

(Underlines represent the restriction recognition sequences for NheI and EcoRI, respectively)

Similarly, WT-Cx40 or Q58L-Cx40 cDNAs were PCR-amplified by the primers Cx40-F8 and Cx40-R3, and the PCR products were digested with XbaI/NotI and subcloned in the lower multiple cloning sites XbaI/NotI of pIRES.

Forward (Cx40-F8) 5'-GCTCTAGACACCATGGGCGATTGGAGC TTCCT-3'

Reverse (Cx40-R3) 5'-ATAAGATGCGGCCGCTCACACTGATAGGTCATCTG-3'

(Underlines represent the restriction recognition sequences for XbaI and NotI, respectively)

Translation rate of the upstream cloned gene is generally greater than that cloned at the downstream site. Expression levels of WT-Cx40 (40 kDa) and Q58L-Cx40-GFP (67 kDa) are determined by western blotting using ant-Cx40 antibody.

3. **Cell culture and transfection**

Connexin 40 constructs were introduced into connexin-deficient HeLa cells or mouse neuroblastoma (N2A) cells, maintained in F-12 or Minimum Essential Medium, respectively, supplemented with 10% fetal bovine serum. HeLa and N2A cells were transfected with plasmids using Lipofectamine LTX or Lipofectamine 2000 (Invitrogen) as per the manufacturer's protocol.

4. **Electrophysiology**

Gap junction currents from heterologously expressed N2A cell pairs were recorded using whole-cell double patch clamp techniques as previously described.[9,10] Recordings were carried out independently in each cell of a pair using two Axopatch 200B amplifiers (Axon Instruments). Current signals were filtered at 100-200 Hz and digitally sampled at 1-2 KHz

using an analog-to-digital interface (Digidata 1322A, Axon Instruments). The data were analyzed using Clampfit 9.2 (Axon Instruments) and Origin 7.5 (Origin Lab). The external solution contained (in mmol/L) 160 NaCl, 10 CsCl, 2 $CaCl_2$, 0.6 $MgCl_2$ and 10 HEPES, at pH 7.4. The intracellular (pipette) solution contained (in mmol/L) 130 $CsCl_2$, 0.5 $CaCl_2$, 10 HEPES, 10 EGTA, 2 Na_2ATP and 3 MgATP (added daily), (pH = 7.2). Pipette resistance was 5-10 MΩ. Octanol was added directly to the external solution at the final concentration of 1 mmol/L at each experiment. Experiments were carried out at room temperature (20-22 ºC). All the chemicals were purchased from Sigma or Wako (Tokyo, Japan).

Gap junction channel conductance (g_j) was determined by conventional methods. Briefly, both cells in the pair ($cell_1$ and $cell_2$) were independently voltage-clamped at the same holding potential (-40 mV). $Cell_1$ was then stepped to a new voltage, thus creating a potential difference across the junction (V_j). The current in $cell_2$ was considered equal and opposite to the junctional current (I_j), and g_j was measured from the ratio I_j/V_j. The pulses were 2 or 5 sec in duration with an interpulse interval of 15 sec. Unitary conductance was obtained from pairs where only one or two functional channels were spontaneously detected. In some cases, cells were uncoupled by exposure to 1 mmol/L octanol. Histograms of events were obtained from channels recorded during repetitive 10-20 sec steps to V_j= +60 mV. To measure unitary conductance, only junctional current traces with events that lasted for longer than 20 ms were included.[9,10] All-points histograms of digitized current traces and the frequency distribution histograms were constructed using Origin 7.5.

To analyze the electrophysiological properties of heterotypic gap junctions consisting of Cx40-WT and Cx40-Q58L, N2A cells were transiently transfected with either Cx40-WT (pIRES2-EGFP plasmid) or Cx40-Q58L (pIRES2-DsRED2 plasmid). Sixteen hours later, both cells were split with trypsin/EDTA and co-cultured. On the following day, the

heterotypic cell pairs of Cx40-WT (green) and Cx40-Q58L (red) were visually identified under fluorescent microscopy. Experiments were carried out at room temperature (20-22 ºC).

5. Immunocytochemistry

HeLa cells were cultured on a glass-bottom dish (Asahi Techno Glass, Chiba, Japan) and transfected with the fusion plasmids of pEGFPN1-Cx40-WT, pCMV-FLAG-Cx40-Q58L, or both. Next day, the cells were washed with phosphate-buffered saline (PBS), fixed in PBS containing 2% formaldehyde for 30 min at 4 °C, and permeabilized with 0.05% Triton X-100 for 30 min at 4 °C. After blocking with PBS containing 4% bovine serum albumin for 1 h at room temperature, the cells were stained with anti-FLAG M2 antibody (mouse monoclonal, 1:200, Sigma) for 1 h at room temperature. Protein reacting with antibody was visualized with Alexa 546-labeled secondary antibody (goat, 1:300, Invitrogen). EGFP and Alexa 546 fluorescence images were recorded with a FluoView FV1000 confocal microscope (Olympus Co, Tokyo) with a 60x oil immersion objective.

6. Western blotting

N2A cells maintained in a 6 well dish were transiently transfected with 3 μg Cx40 plasmids. Two days after transfection, cells were washed with PBS, and total cell lysate was extracted with lysis buffer including 50 mM Tris (pH7.5), 150 mM NaCl, 1% TritonX-100, 0.1 μg/ml aprotinin, 1x complete protease inhibitor (Roche Applied Science). Lysates precleared by centrifugation at 15,000 xg for 10 min were subjected to SDS-PAGE and immunoblotting with rabbit anti-Cx40 antibody (Millipore). Proteins reacting with primary antibodies were visualized by ECL system (GE Healthcare). The membrane was reprobed by anti-GAPDH antibody (Sigma).

7. Surface biotinylation

HeLa cells plated on 100 mm dishes were transiently transfected with 11 μg of pEGFPN1-Cx40-Q58L using Lipofectamine 2000 (Invitrogen). Surface biotinylation was performed 48 hours after transfection using the Pierce Cell Surface Protein Isolation Kit (Thermo Scientific, #89881) as per the manufacturer's protocol. Briefly, after 30 min of biotin labeling reaction at 4 °C, cell were lysed, mixed with NeutrAvidin agarose, and loaded on a column. The biotinylated proteins were eluted with the elution buffer. Fractions of the flowthrough, elute, and input lysate (1:1 diluted with lysate buffer) were subjected to a 4-12% gradient SDS-PAGE and immunobotting with anti-Cx40 antibodies (Cx40-A, 1:50 dilution, Alpha Diagnostic International). Proteins reacting with primary antibodies were visualized by LI-COR infrared imaging technology. Detection was done using anti-rabbit IRDye 800CW (1:10,000) antibodies (LI-COR Biosciences, # 926-32213).

8. Functional evaluation of novel *SCN5A* mutations associated with PFHB1

Three novel *SCN5A* mutations associated with PFHB1 were identified; a missense mutation F777L, a compound heterozygous frame shift mutation p.P701fsX710 plus p.P2006fsX2037, and a frame shift mutation pV1764fsX1786. These mutations were not found in 400 unaffected control alleles. Functional properties of these mutations were evaluated by whole-cell patch clamp. The mammalian expression plasmids encoding the mutations were constructed by site-directed mutagenesis as we described previously using a human Na channel α subunit (Nav1.5) cDNA.[11] The human cell line tsA-201 was transiently transfected together with Na channel β1 subunit, and the whole-cell Na currents were recorded as we previously described.[11] Electrode resistance ranged from 0.8 to 1.5 MΩ. Data

acquisition was carried out using an Axopatch 200B patch clamp amplifier and pCLAMP10 software (Axon Instruments). Currents were filtered at 5 kHz (–3 dB; 4-pole Bessel filter) and digitized using an analog-to-digital interface (Digidata 1440A; Axon Instruments). Experiments were carried out at room temperature (20–22°C). Voltage errors were minimized using series resistance compensation (generally 80%). Cancellation of the capacitance transients and leak subtraction were performed using an online P/4 protocol. The pulse protocol cycle time was 10 s. The data were analyzed using Clampfit 10 (Axon Instruments) and SigmaPlot 11 (SPSS Science). The holding potential was –120 mV. The bath solution contained (in mmol/l): 145 NaCl, 4 KCl, 1.8 $CaCl_2$, 1 $MgCl_2$, 10 HEPES, and 10 glucose, pH 7.35 (adjusted with NaOH). The pipette solution (intracellular solution) contained (in mmol/l): 10 NaF, 110 CsF, 20 CsCl, 10 EGTA, and 10 HEPES, pH 7.35 (adjusted with CsOH). The time from establishing the whole-cell configuration to onset of recording was consistent cell-to-cell to exclude the possible time-dependent shift of steady-state inactivation. To determine activation parameters, the current-voltage relationship was fit to the Boltzmann equation $I = (V - V_{rev}) \times G_{max} \times (1 + \exp[V - V_{1/2}] / k)^{-1}$, where I is the peak Na current during the test pulse potential V. The parameters estimated by the fitting are V_{rev} (reversal potential), G_{max} (maximum conductance), and k (slope factor) (Supplemental Figure 1B). Steady-state availability for fast inactivation was measured with a standard double-pulse protocol (Supplemental Figure 1C, left inset), and the data were fit with the Boltzmann equation $I/I\text{max} = (1 + \exp[(V - V_{1/2}) / k])^{-1}$, where I_{max} is the maximum peak Na current, to determine the membrane potential for $V_{1/2}$ and k. Functional properties of other mutations in *SCN5A* or *SCN1B* were previous reported (Supplemental table S1).

SUPPLEMENTAL FIGURE LEGEND

Supplemental Figure S1

Functional properties of the novel *SCN5A* mutations

Panel A shows whole-cell Na currents recorded from tsA201cells expressing wild type (WT) Nav1.5 (left) or Nav1.5 mutant F777L (right). Currents were elicited by step pulses from -90 mV to +60 mV (10 mV step) from a holding potential of -120 mV. Bars: 5 msec and 2 nA. Non-inactivated late currents were not observed. Panel B shows current-voltage relationship. Average peak current density was significantly reduced in F777L ($p<0.001$). WT: 391.7±47.1 pA/pF, n=15 (open circles). F777L: 301.2±30.0 pA/pF, n=9 (closed circles). Panel C shows that the voltage-dependence of activation of F777L channels (closed circles) was not different from control, whereas steady-state inactivation curve was significantly shifted in the hyperpolarizing direction in F777L (WT: $V_{1/2}$= -87.1±0.5 mV, n=25; F777L: $V_{1/2}$= -92.4 ± 1.3 mV, n=9; $p<0.001$). These biophysical properties suggest a decrease in the number of functional (conductive) sodium channels during the action potential upstroke consequent to the mutation. Previous studies have revealed that mutations A1180V[12] and D1275N[13], also found in our series (see supplemental Table S1), exhibit minor functional abnormalities when expressed in cultured cells, though more drastic changes are observed when the channels are expressed in cardiomyocytes[14]. Cells expressing compound heterozygous mutations p.P701fsX710 and p.P2006fsX2037, or a frame shift mutation pV1764fsX1786, exhibited no Na current, suggesting haploinsufficiency of cardiac Na current in the afflicted population.

Supplemental Figure S2

Exercise stress test of the proband's mother

Electrocardiographic recording obtained from the probands's mother during a treadmill exercise stress test at the age of 16. A heart rate of 177 bpm was achieved after 9 min 20 sec of exercise test by Bruce protocol. During the recovery phase at 1 min 17 sec, superior axis narrow QRS ventricular tachycardia with a rate of 110 bpm was observed (upper panel) .Ventricular tachycardia was spontaneously terminated at 20 min 23 sec of the recovery phase (lower panel).

Supplemental Figure S3

Co-expression of Cx40-WT and Cx40-Q58L in N2A cells.

Panels A-C show fluorescence images from a cell pair recorded from cells co-transfected with pIRES2-EGFP-Cx40-WT and pIRES2-DsRED2-Cx40-Q58L (0.5 μg each). Notice expression of both the green (A) and the red marker (B), giving a yellow color in the overlay (C). Calibration bar: 20 μm. Panel D: Junctional conductance recorded from cell pairs as that shown in panels A-C was 18.9±5.4 nS (n=6). This number was not statistically different from that obtained from pairs expressing WT-GFP and Q58L-GFP (average Gj= 13.0±2.4 nS; n=17).

Supplemental Figure S4

Surface biotinylation of Q58L-Cx40 expressed in HeLa cells.

HeLa cells transfected with pEGFPN1-Cx40-Q58L were surface-labeled with biotin, and lysed. Cell lysate was mixed with NeutrAvidin agarose and loaded on a column. Flowthough, elute (biotin-labeled membrane fraction) and the input lysate (1:1 diluted with lysate buffer) were subjected to SDS-PAGE and immunoblotting. A single 67KDa band of similar intensity

was detected in both elute and the input lysate, but not in the flowthrough. These data indicate that mutation Q58L did not prevent surface expression of the Cx40 protein.

SUPPLEMENTAL REFERENCES

1. Wang Q, Li Z, Shen J, Keating MT. Genomic organization of the human SCN5A gene encoding the cardiac sodium channel. *Genomics*. 1996;34:9-16
2. Splawski I, Shen J, Timothy KW, Lehmann MH, Priori S, Robinson JL, Moss AJ, Schwartz PJ, Towbin JA, Vincent GM, Keating MT. Spectrum of mutations in long-QT syndrome genes. KVLQT1, HERG, SCN5A, KCNE1, and KCNE2. *Circulation*. 2000;102:1178-1185
3. Plaster NM, Tawil R, Tristani-Firouzi M, Canun S, Bendahhou S, Tsunoda A, Donaldson MR, Iannaccone ST, Brunt E, Barohn R, Clark J, Deymeer F, George AL, Jr., Fish FA, Hahn A, Nitu A, Ozdemir C, Serdaroglu P, Subramony SH, Wolfe G, Fu YH, Ptacek LJ. Mutations in Kir2.1 cause the developmental and episodic electrical phenotypes of Andersen's syndrome. *Cell*. 2001;105:511-519.
4. Makita N, Sloan-Brown K, Weghuis DO, Ropers HH, George AL, Jr. Genomic organization and chromosomal assignment of the human voltage-gated Na^+ channel beta 1 subunit gene (SCN1B). *Genomics*. 1994;23:628-634
5. Watanabe H, Koopmann TT, Le Scouarnec S, Yang T, Ingram CR, Schott JJ, Demolombe S, Probst V, Anselme F, Escande D, Wiesfeld AC, Pfeufer A, Kaab S, Wichmann HE, Hasdemir C, Aizawa Y, Wilde AA, Roden DM, Bezzina CR. Sodium channel beta1 subunit mutations associated with Brugada syndrome and cardiac conduction disease in humans. *J. Clin. Invest.* 2008;118:2260-2268
6. Medeiros-Domingo A, Kaku T, Tester DJ, Iturralde-Torres P, Itty A, Ye B, Valdivia C, Ueda K, Canizales-Quinteros S, Tusie-Luna MT, Makielski JC, Ackerman MJ. *SCN4B*-encoded sodium channel β4 subunit in congenital long-QT syndrome. *Circulation*. 2007;116:134-142

7. Schulze-Bahr E, Neu A, Friederich P, Kaupp UB, Breithardt G, Pongs O, Isbrandt D. Pacemaker channel dysfunction in a patient with sinus node disease. *J. Clin. Invest.* 2003;111:1537-1545

8. Britz-Cunningham SH, Shah MM, Zuppan CW, Fletcher WH. Mutations of the connexin43 gap-junction gene in patients with heart malformations and defects of laterality. *New Engl. J. Med.* 1995;332:1323-1330

9. Seki A, Coombs W, Taffet SM, Delmar M. Loss of electrical communication, but not plaque formation, after mutations in the cytoplasmic loop of connexin43. *Heart Rhythm*. 2004;1:227-233

10. Anumonwo JMB, Taffet SM, Gu H, Chanson M, Moreno AP, Delmar M. The carboxyl terminal domain regulates the unitary conductance and voltage dependence of connexin40 gap junction channels. *Circ. Res.* 2001;88:666-673

11. Makita N, Behr E, Shimizu W, Horie M, Sunami A, Crotti L, Schulze-Bahr E, Fukuhara S, Mochizuki N, Makiyama T, Itoh H, Christiansen M, McKeown P, Miyamoto K, Kamakura S, Tsutsui H, Schwartz PJ, George AL, Roden DM. The E1784K mutation in SCN5A is associated with mixed clinical phenotype of type 3 long QT syndrome. *J. Clin. Invest.* 2008;118:2219-2229

12. Ge J, Sun A, Paajanen V, Wang S, Su C, Yang Z, Li Y, Wang S, Jia J, Wang K, Zou Y, Gao L, Wang K, Fan Z. Molecular and clinical characterization of a novel SCN5A mutation associated with atrioventricular block and dilated cardiomyopathy. *Circ Arrhythmia Electrophysiol*. 2008;1:83-92

13. Groenewegen WA, Firouzi M, Bezzina CR, Vliex S, van Langen IM, Sandkuijl L, Smits JP, Hulsbeek M, Rook MB, Jongsma HJ, Wilde AA. A cardiac sodium channel mutation cosegregates with a rare connexin40 genotype in familial atrial standstill.

Circ. Res. 2003;92:14-22

14. Watanabe H, Nogami A, Ohkubo K, Kawata H, Hayashi Y, Ishikawa T, Makiyama T, Nagao S, Yagihara N, Takehara N, Kawamura Y, Sato A, Okamura K, Hosaka Y, Sato M, Fukae S, Chinushi M, Oda H, Okabe M, Kimura A, Maemura K, Watanabe I, Kamakura S, Horie M, Aizawa Y, Shimizu W, Makita N. Electrocardiographic Characteristics and SCN5A Mutations in Idiopathic Ventricular Fibrillation Associated with Early Repolarization. *Circulation: Arrhythmia and Electrophysiology*. 2011

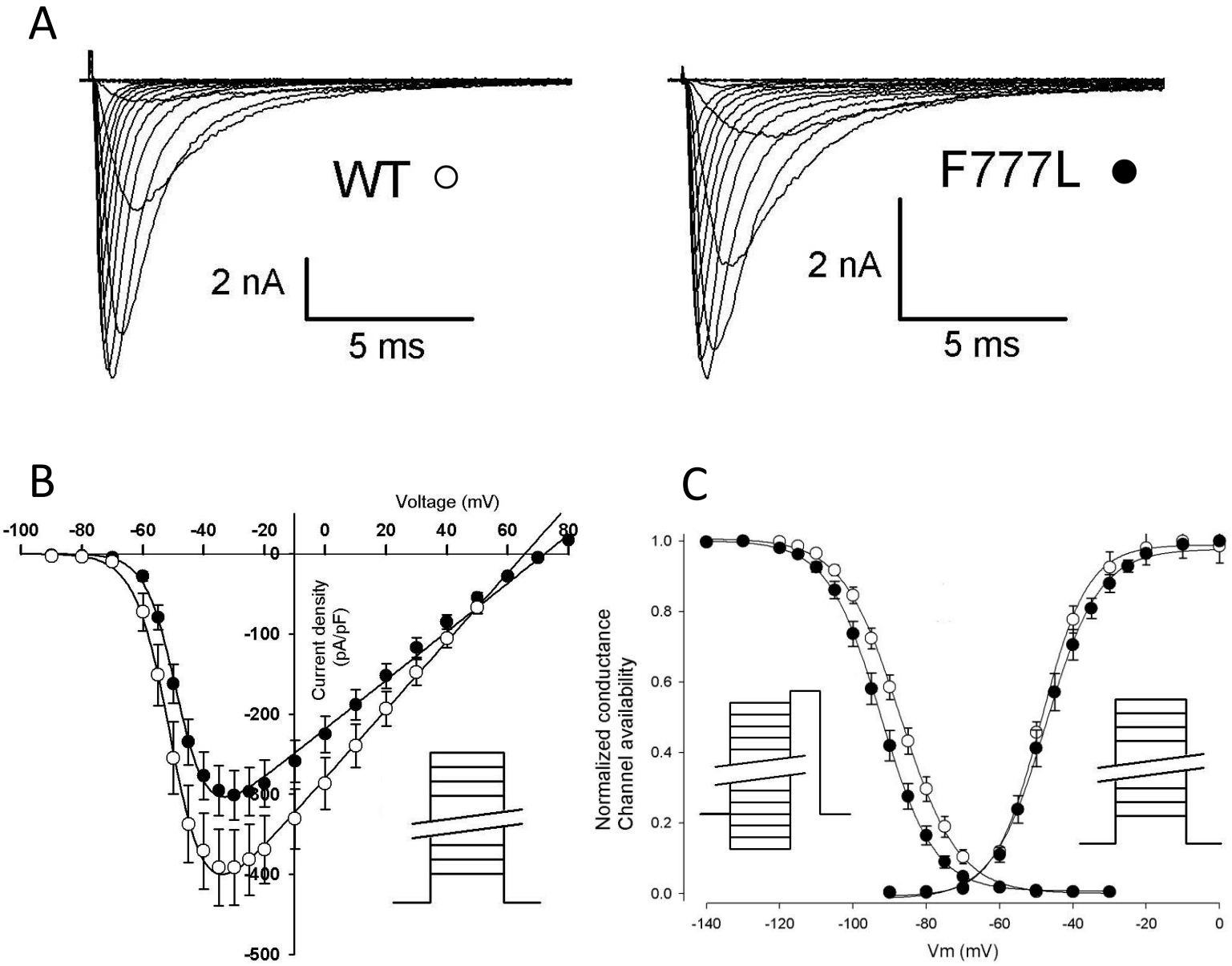

VT initiation at 1’17” (recovery phase)

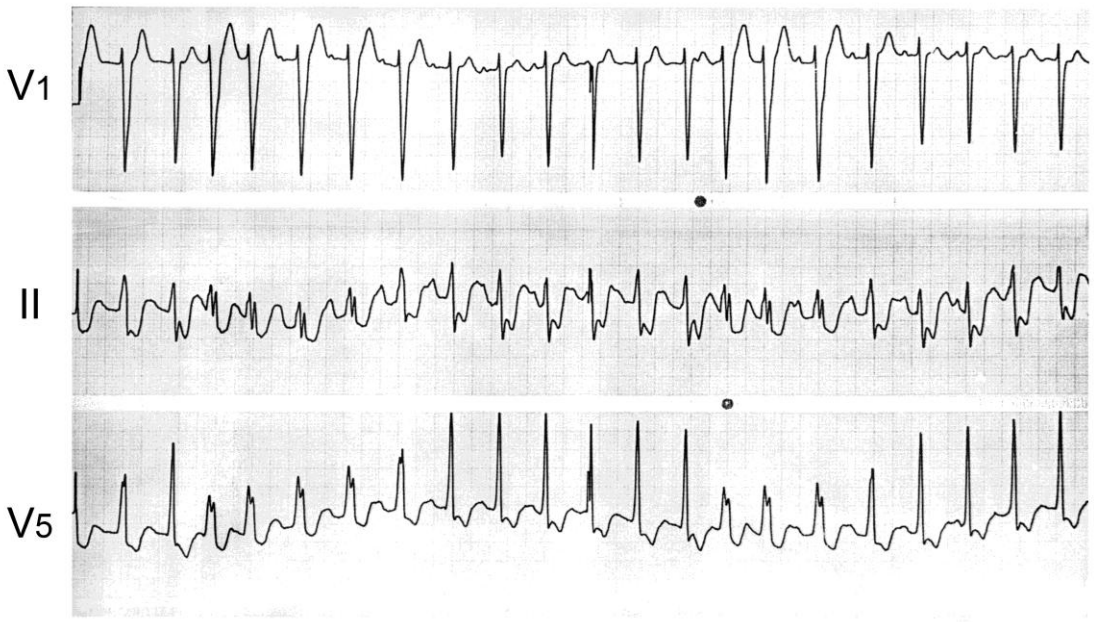

Spontaneous VT termination at 20’23”

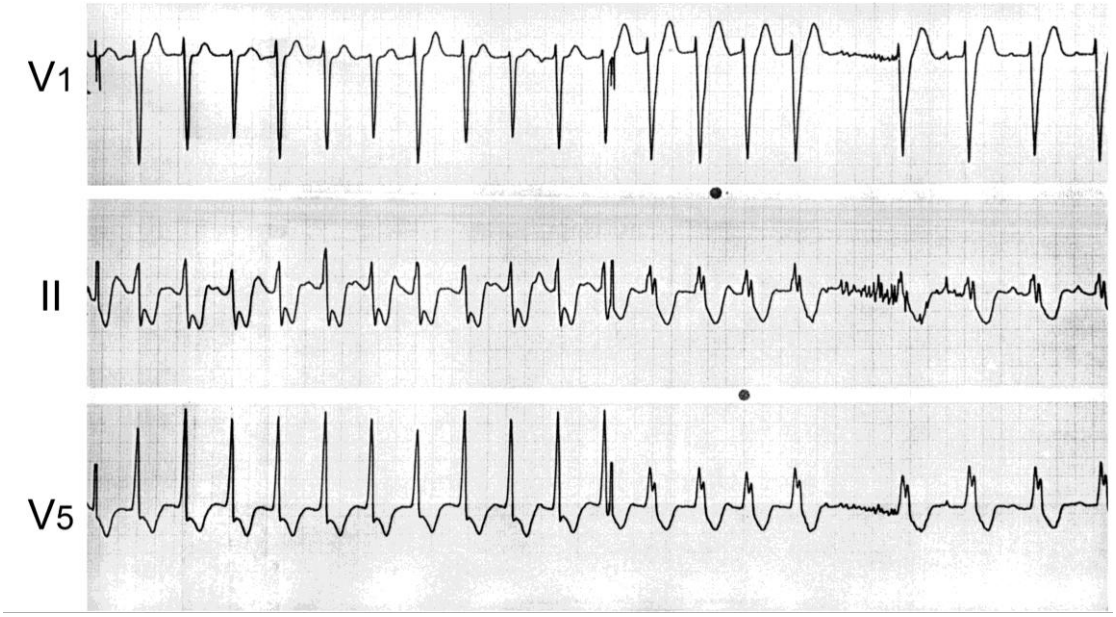

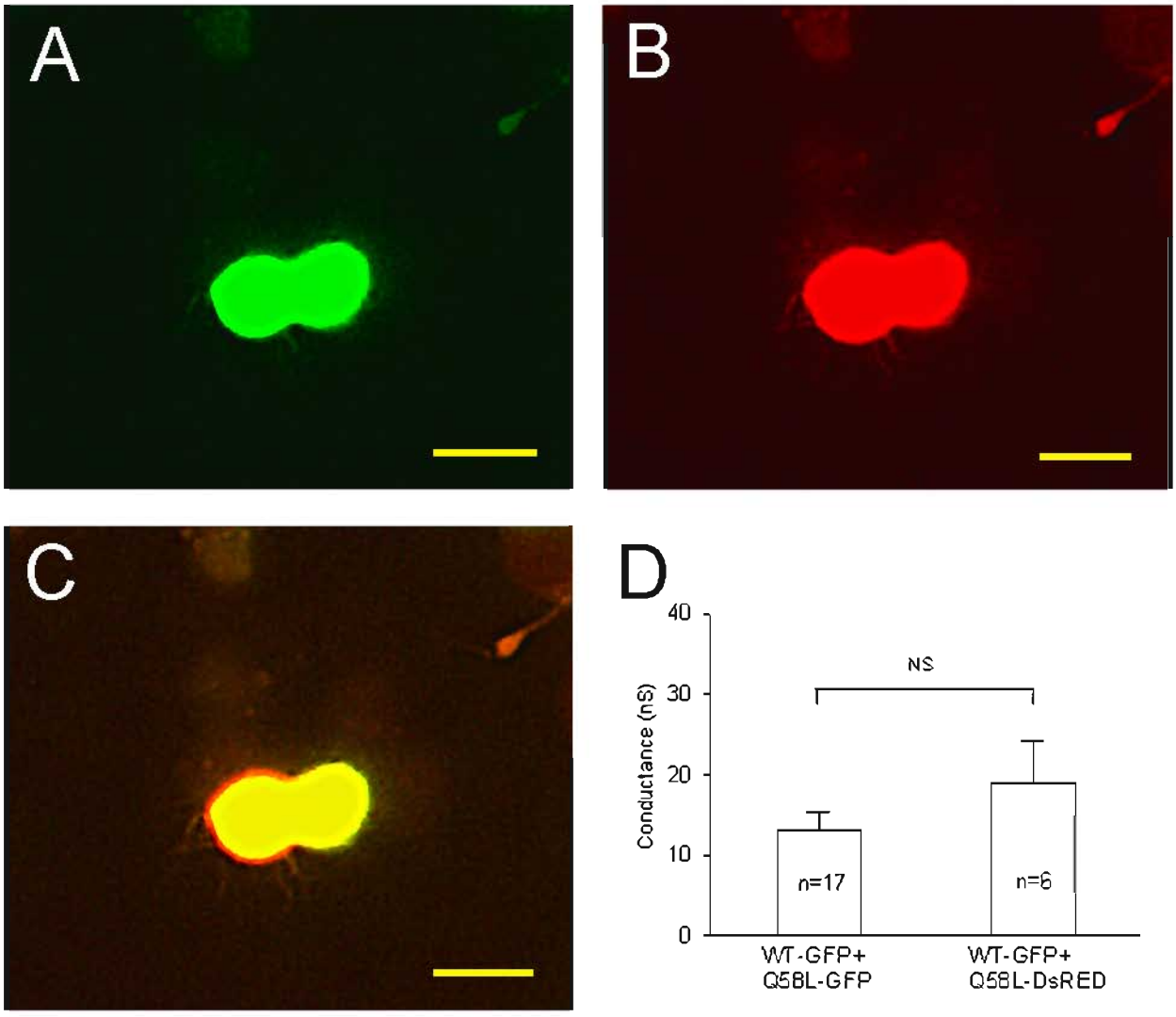
A
B
C
D
40
30
20
10
0
Conductance (nS)
NS
n=17
n=6
WT-GFP+
Q58L-GFP
WT-GFP+
Q58L-DsRED

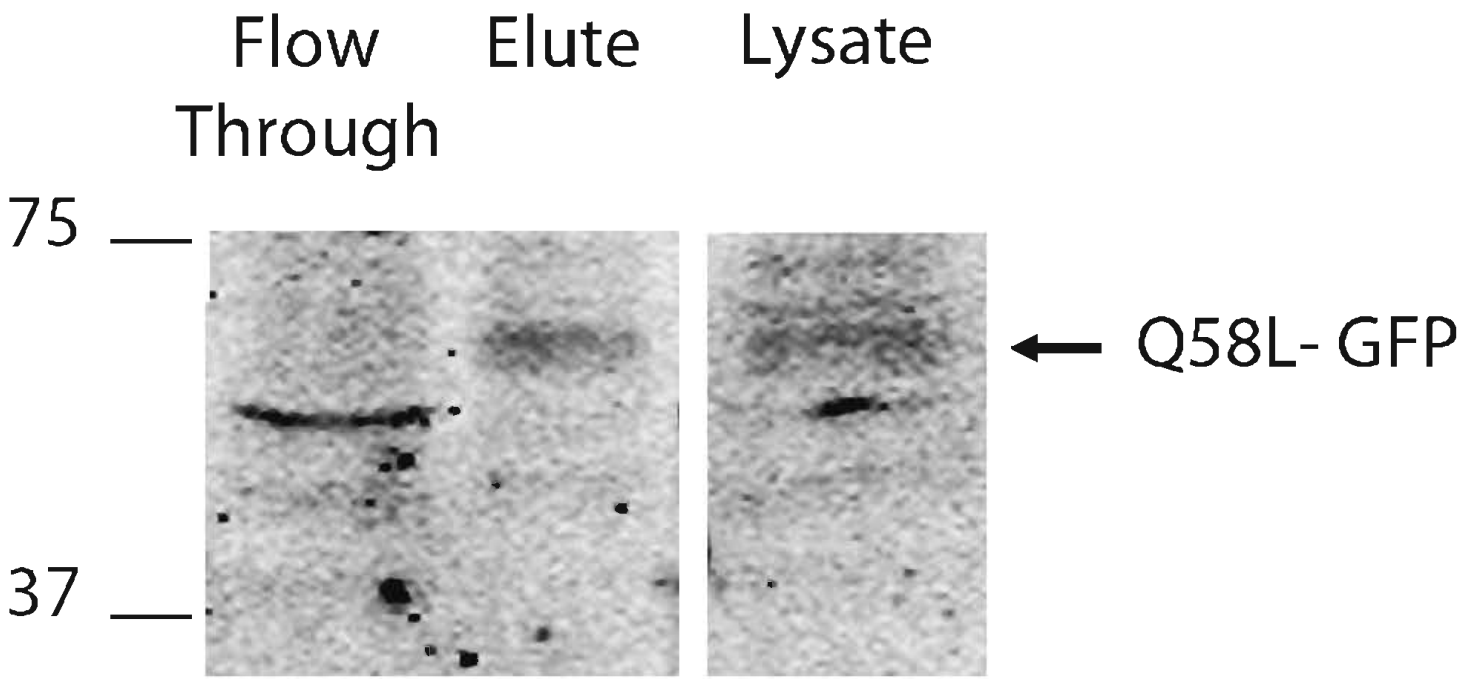

Supplemental Table S1. Genetic mutations identified in PFHBI probands

Patient	Gene	Exon	cDNA mutation	Amino acid change	Mutation type	Phenotype	Reference
1 †	*GJA5*	2	c.173 A>T	Q58L	Missense	PFHBI	this study
2	*SCN5A*	15	c.2329T>C	F777L	Missense	PFHBI +DCM+MMD	this study
3 †*	*SCN5A*	14	c.2102 del C	p.P701fsX710	Deletion	PFHBI +BrS	this study
	SCN5A	28	c.6017 delC	p.P2006fsX2037	Deletion		this study
4	*SCN5A*	28	c.5290 delG	p.V1764fsX1786	Deletion	PFHBI +BrS+MMD	this study
5	*SCN5A*	20	c.3539C>T	A1180V	Missense	PFHBI +DCM	[11]
6	*SCN5A*	21	c. 3823G>A	D1275N	Missense	PFHBI +DCM	[12]
7	*SCN5A*	Int22	IVS22+2T>C		Exon skipping	PFHBI	[13]
8	*SCN5A*	28	c.5280 delG	p.A1711fsX1786	Deletion	PFHBI	[13]
9	*SCN5A*	28	c. 5129C>T	S1710L	Missense	PFHBI +IVF	[14]
10	*SCN1B*	3	c.259G>C	E87Q	Missense	PFHBI	[5]
11	*SCN1B*	3A	c.536G>A	W179X	Missense	PFHBI+BrS	[5]
12	*SCN1B*	3A	c.537G>A	W179X	Missense	PFHBI	[5]

GJA5: connexin 40, *SCN5A*: cardiac voltage-gated Na channel α subunit, *SCN1B*: voltage-gated Na channel β1 subunit

†: Patients 1 and 3 are sudden cardiac death victims

*: Patient 3 is a compound heterozygous carrier of *SCN5A* mutations

DCM: dilated cardiomyopathy, MMD: myotonic muscular dystrophy, BrS: Brugada syndrome, IVF: idiopathic ventricular fibrillation, Int22: Intron 22

Supplemental Table S2. ECG parameters of the family members

Family	Age	HR (bpm)	PR (ms)	QRS (ms)	QTc (ms)	Axis (degree)	ST depression
Proband	6	87	*	126	421	-8	II,III,aVF, V3-6
	8	77	*	128	396	-21	II,III,aVF, V2-6
Sister	6	86	130	86	404	-25	II,III,aVF, V3-6
	11	85	142	88	416	-49	II,III,aVF, V3-6
Mother	16	63	248	152	471	-25	II,III,aVF, V3-6

*: advanced AV block